Excimer Formation and Energy Trapping in Langmuir–Blodgett Films of Poly(vinyl octal) Containing Pyrene Chromophore

Satoru Ohmori, Shinzaburo Ito, and Masahide Yamamoto*

Department of Polymer Chemistry, Faculty of Engineering, Kyoto University, Sakyo-ku, Kyoto 606, Japan

Received December 1, 1989; Revised Manuscript Received February 22, 1990

ABSTRACT: Mono- and multilayered films of poly(vinyl octal) containing pyrene chromophore have been prepared by the Langmuir–Blodgett (LB) technique. The photophysical processes, excimer formation and energy trapping of pyrene chromophore in the 2-dimensional and quasi 3-dimensional systems, have been investigated by photostationary and time-resolved fluorescence spectroscopy. Monolayered films of the polymer on pure water were transferred to a quartz plate at 19 °C as a Y-type film. UV absorbance and fluorescence intensity of the built-up films were proportional to the number of layers. The obtained films show little excimer emission. The ratio of excimer fluorescence to the monomer fluorescence is much less than that of mixed films fabricated from a conventional fatty acid with pyrene chromophore, at the same concentration of the chromophore in a plane. Fluorescence decay analysis by a 2-dimensional energy-transfer model gives the density of excimer-forming sites. The results indicate that the polymer LB films attain a statistically uniform distribution of pyrene moieties. In multilayered films, the decay curves did not fit to the Förster kinetics in which energy migration is not involved, and they were analyzed by the Yokota–Tanimoto Padé model involving migration of the excited state among pyrene moieties. The diffusion coefficient for the energy migration was found to be 1×10^{-6} cm^2 s^{-1}. The observed characteristics of the polymer LB films are attributed to the uniform distribution of pyrene moieties and the thin thickness of each layer.

Introduction

The Langmuir–Blodgett (LB) method is one of the most powerful techniques for realizing artificial molecular assemblies. This method enables us to design the spatial arrangement of organic molecules in the dimension of molecular size. This means that fundamental photoprocesses such as excitation energy-transfer and electron-transfer processes can be controlled by the designed structure of LB films. Because of the fascinating features, extensive studies on LB films have been conducted after the pioneering works of Kuhn and his co-workers.[1] Those studies have revealed the advantages and disadvantages of the conventional LB films, consisting usually of long-chain fatty acids.

Recently, Yamazaki et al. performed a fine investigation on chromophore distributions in mixed LB films by means of picosecond fluorescence decay analysis.[2-3] In their system, the amphiphilic pyrene moieties were dispersed in the LB film of long-chain fatty acids but the chromophore formed aggregates or ground-state dimers of pyrene units.[3] They found uniform distribution of pyrene moieties in a plane of LB film difficult to obtain.

Another disadvantage of the LB films of fatty acids is the thermal and mechanical instability. Some investigators made LB films stable by polymerization of a monolayer or multilayers containing a polymerizable group.[4-13] Recently some preformed polymers were found to form a stable monolayer at the air–water interface and to be transferable to solid substrates.[13-25] One of these polymers is poly(vinyl alkanal), which has been reported by Ogata et al.[25] This polymer is prepared by the acetalization of poly(vinyl alcohol) with alkylaldehydes. To this polymer can be easily introduced various kinds of functional groups by the coexistence of chromophoric aldehydes with alkylaldehyde in the acetalization.[26]

Excimer formation and energy trapping of chromophores in polymer solids depend on the chromophore distribution in the polymer matrices. Recently, we succeeded in preparing the polymer having a carbazole chromophore in which the moieties are uniformly distributed in the solid film. The polymer was made by the copolymerization of the carbazole-containing monomer with an inert comonomer.[27]

In this study, to obtain stable LB film having controlled chromophore distribution in a plane,[27] pyrene chromophore was introduced to a preformed polymer poly(vinyl octal) by a polymer reaction, and the LB films of these copolymers were prepared. The excimer formation and energy-trapping processes of pyrene moieties in the polymer LB films were investigated by photostationary and time-resolved fluorescence spectroscopy.

Experimental Section

Sample Preparation. Poly(vinyl octal) with pyrene chromophore was synthesized by acetalization of commercial poly(vinyl alcohol) (PVA) (Wako Pure Chemical Industries, Ltd.; DP 2000), according to the procedure of Ogata et al.[25] PVA powder (1 g) and a mixture of octanal (Wako Pure Chemical) and pyrenecarbaldehyde (Aldrich Chemical) (60 mmol) were dissolved in 16 mL of benzene and 4 mL of ethanol, and 2 drops of hydrochloric acid was added as the catalyst. The reaction mixture was stirred for 15 h at 40 °C. PVA powder dissolved as the acetalization proceeded. The solution was poured into 1 L of methanol containing a trace amount of sodium hydroxide. The polymer was purified by reprecipitation from benzene into methanol three times and dried in vacuo.

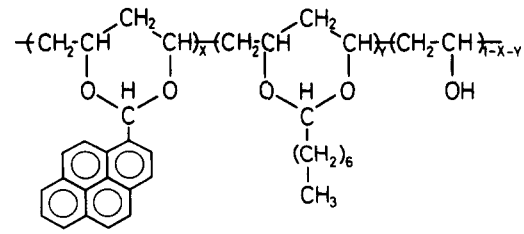

Table I shows the feed ratios of two kinds of aldehydes. The fractions of octal unit and pyrene unit in the obtained polymer were calculated from UV absorbance in dichloromethane and from the carbon fraction obtained by elemental analysis. The extinction coefficient of pyrene chromophore used in the calculation is 42 500 L mol^{-1} cm^{-1} at 344 nm, which is determined

0024-9297/90/2223-4047$02.50/0

Table I
Amount of Reactant Aldehydes, Composition of Polymer, Glass Transition Temperature of Copolymers, Average Distance between Pyrene Moieties in a Monolayer and Limiting Area of Acetal Units

sample	octanal, g	pyrenecarbaldehyde, g	X, %	Y, %	$X/(X+Y)$, %	T_g, °C	r_{Py-Py} in 2D, nm	area of acetal, nm²/unit
P0	8.0	0.00	0.0	73.0	0.0	25		0.36
P1	8.0	0.10	0.14	64.8	0.2	28	12.8	0.36
P2	7.6	0.72	1.35	64.7	2.0	31	4.15	0.35
P3	7.2	1.48	2.91	60.3	4.6	35	2.80	0.36
P4	6.4	2.87	5.58	56.3	9.0	45	2.03	0.35
P5	4.0	7.40	9.07	63.6	12.5	50	1.70	0.36

by pyrenemethanol as a model compound. Although the reactivity of pyrenecarbaldehyde is about half of that of octanal, the pyrene units were introduced up to 12.5% of acetal units (P5). The samples up to $X/(X+Y) = 9\%$ could be obtained in the same reaction condition; the ratio of acetalized units $(X+Y)$ to the whole units decreased from 73% (P0) to 62% (P4) with the increase of pyrene content, owing to the low reactivity of pyrenecarbaldehyde. The reaction was forced to a severe condition to obtain the polymer (P5) having higher pyrene concentration than P4: the reaction was continued for 37 h, and the solvent was increased to 30 mL (24 mL of benzene and 6 mL of ethanol), in order to dissolve the pyrenecarbaldehyde. The T_g's of these polymers increased with an increase of pyrene concentration. Table I also shows the average distance between two pyrene moieties in a monolayer assuming a uniform distribution. The values were calculated from surface pressure–area isotherms.

The benzene solution of the acetalized polymer (0.01 wt %) was spread on the surface of pure water in a Langmuir trough. The water used in the subphase was purified by deionization, distillation, and then passing through a water purification system (Barnstead Nanopure II). The spread polymer was compressed at the rate of 1 cm min^{-1} at 19 °C. The surface pressure–area isotherm (F–A isotherm) was recorded by using a Wilhelmy type film balance (Shimadzu ST-1). The substrate was a nonfluorescent quartz plate (1 cm × 4 cm), which was cleaned in sulfuric acid containing a small amount of potassium permanganate, dipped in a 10% hydrogen peroxide solution, and then washed by pure water and made hydrophobic by dipping it in a 10% solution of trimethylchlorosilane for 20 min. In order to remove the effect of the interface of substrate, four layers of poly(vinyl octal) (P0) were deposited on the substrate beforehand. After the deposition of chromophoric polymer, four layers of P0 were again deposited to avoid the effect of the air interface. During the deposition, the surface pressure of the spread film was controlled to an adequate value for each polymer (25 mN m^{-1} for P0–P4 and 20 mN m^{-1} for P5). The film was transferred by dipping the quartz plate vertically at the rate of 2 cm min^{-1}. Cast films on quartz plates were also prepared from a toluene solution of polymer (1 wt %) by a spin-coating method at 5000 rpm for 90 s.

Measurements. UV absorption spectra were measured by a Shimadzu UV-200S. Fluorescence spectra and excitation spectra were recorded by a Hitachi 850 fluorescence spectrophotometer. A single-photon-counting method was used for the measurements of fluorescence decay curves and time-resolved fluorescence spectra.[28] The pulsed excitation light was obtained with a Spectra-Physics picosecond synchronously pumped, modelocked, cavity-dumped dye laser (Models 2020, 342A, 375B, and 344S). The emission through a diffuser and monochromator was detected with a microchannel-plate photomultiplier (Hamamatsu R1564U-01).[29] The time-correlated pulses were obtained by conventional Ortec photon-counting electronics and accumulated on a multichannel analyzer (Norland IT-5300) controlled with a microcomputer (NEC 9801). The full-width at half-maximum of the overall excitation pulse was 75 ps. The spectral response was calibrated with a standard tungsten lamp. The obtained fluorescence decay was analyzed by the least-squares method using a computer (NEC 9801). To eliminate the polarization effect on the fluorescence decay curves, magic angle excitation was adopted according to Weber et al.[30] The glass transition temperature of the copolymers was measured by a differential scanning calorimeter (Mettler FP 85).

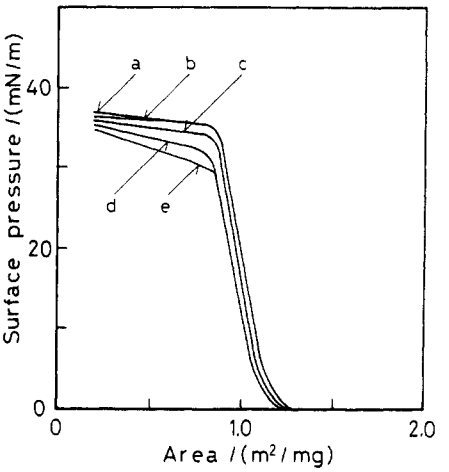

Figure 1. Surface pressure–area isotherms of poly(vinyl octal) containing pyrene moieties: (a) P0, (b) P2, (c) P3, (d) P4, (e) P5.

Results and Discussion

Surface Pressure–Area Isotherms and Transfer of Surface Film to Solid Substrate. Figure 1 shows the surface pressure–area isotherms of each polymer. As the surface film is compressed on water, the surface pressure increases sharply at the area of 1 m^2 mg^{-1}. By further compression, the monolayer film begins to collapse at the plateau region of the F–A isotherms. With the increase of the concentration of pyrene moieties from P0 to P5, the surface pressure in the collapsed region (plateau region) decreases from 35 to 30 mN m^{-1} and the limiting area slightly decreases from 1.13 to 1.09 m^2 mg^{-1}. Here the limiting area was obtained by extrapolating the steepest line of the F–A isotherm to zero surface pressure. The decrease of the area is due to the larger molecular weight of the pyrene unit than the octyl one. When the limiting area of poly(vinyl alcohol) unit is assumed to be 0.12 nm^2 unit^{-1},[31] the limiting area of acetalized unit can be calculated as shown in Table I. The areas are between 0.35 and 0.36 nm^2 unit^{-1}, which are independent of the content of pyrene moieties. This value is consistent with the one reported by Ogata for poly(vinyl acetals).[25] From this behavior, there is no problem with the monolayer formation on the water surface and with the deposition to substrates, even if 12.5% of the octyl units are replaced with the pyrene units. In fact, all the polymers are easily transferred to a quartz plate at 20–25 mN m^{-1} at 19 °C. The deposited LB film is Y-type, because the decrease of the surface area on water was equal to the deposited area for both the downward and upward strokes. The results indicate that pyrene moieties can be introduced in the polymer LB films by their attachment as the side chain of the base polymer: poly(vinyl octal).

In order to verify the deposition of the surface film to the substrate, the absorbance and the fluorescence intensity of transferred LB films were measured. Because LB films are very thin, the absorbance for a several layer film is too small to be measured with a sufficient signal to noise ratio.

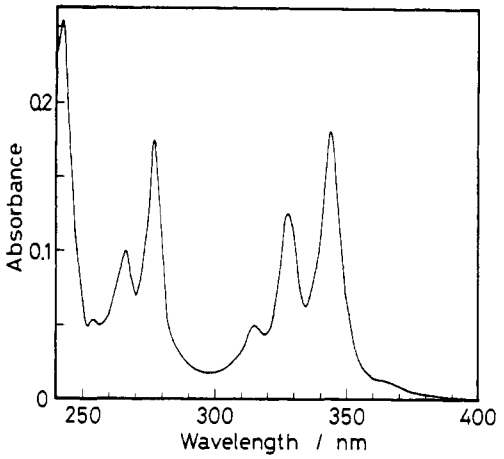

Figure 2. UV absorption spectrum of a 40-layer (on one side) LB film of P5. The absorbance corresponds to an 80-layer film, because the layers are transferred to both sides of a quartz plate.

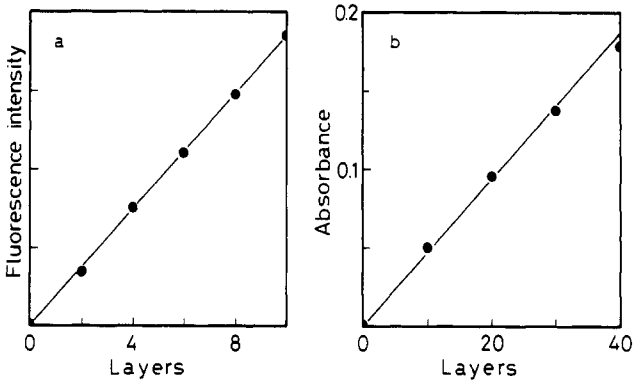

Figure 3. Fluorescence intensity and UV absorbance of built-up films as a function of the number of layers (on one side): (a) fluorescence intensity of P2 and (b) UV absorbance of P5 at 344 nm.

Figure 2 shows the UV absorption spectrum of the 40-layer film on one side of P5. The absorbance corresponds to an 80-layer film, because the layer is transferred to both faces of a quartz plate. Hereafter, the number of layers represents the one on one side of a substrate.

Figure 3a shows the relation between the fluorescence intensity of P2 and the number of layers, where polymer P2 free from excimer emission was chosen. It is clear that the fluorescence intensity increased proportionally with the number of layers. Figure 3b shows the relation between the absorbance of P5 films at 344 nm and the number of layers. This figure also shows a proportional relation. That is, the surface film can be transferred satisfactorily at least up to 40 layers. From the absorbance of the LB films, the plane density of pyrene moieties per single layer is calculated to be 3.4×10^{17} unit m^{-2} assuming the random orientation of pyrene moieties. The assumption is correct as the ratio of the absorbances of L_a and B_b transition ($A_{B_b}/A_{L_a} = 0.97$) does not deviate strongly from the solution value 1.02 and there is not the dichroism of UV absorption. This density of pyrene moieties agrees with the value 3.5×10^{17} unit m^{-2}, which is calculated from the composition of the polymer and the area of the monolayer at the deposition point. The result is consistent with the transfer ratio of unity. This shows that the surface film is stable enough to be transferred to the substrate.

Excimer Formation and Chromophore Distribution. As shown in Figure 2, the UV absorption spectrum shows peaks at 344, 327, and 313 nm, which are the same as those in the spectra of the spin-coated films of the samples of lower pyrene content. This shows that there is no strong

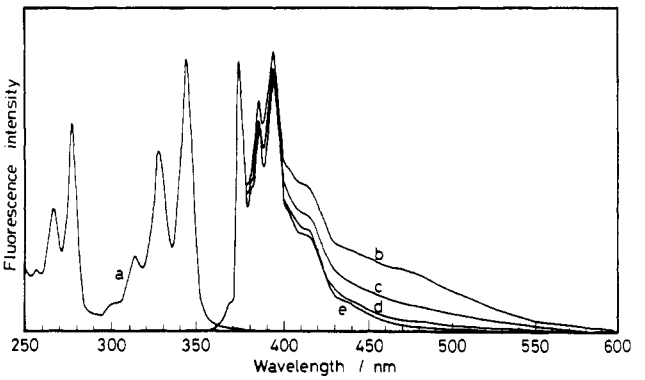

Figure 4. Fluorescence emission spectra of 6-layer (on one side) films of (e) P2, (d) P3, (c) P4, and (b) P5. The spectrum a shows the fluorescence excitation spectrum of a 20-layer film of P5, monitored at 375 nm.

interaction between pyrene moieties in the ground state; even the 12.5% of acetal units are replaced by the pyrene units.

Excimer formation of the pendant pyrene unit was often utilized as a molecular probe for the aggregation of chromophore.[32-34] Figure 4 shows the fluorescence spectra and the excitation spectra of 6-layer films. The emission band at 375, 386, and 395 nm is the monomer fluorescence. In the low pyrene content sample, P1, the shape of the emission spectrum is the same as that of P2. The normal excimer emission at 470 nm, which is usually observed in solution, is observed for the samples of pyrene concentrations above P3. In addition to this emission there is a slight increase of the intensity around 420 nm with an increase of pyrene concentration. This emission is probably due to the partial overlapping excimer whose existence is reported in the LB film of fatty acids, in a vapor-deposited film, in neat liquid, and in a single crystal.[3] Although the pyrene chromophore easily forms the excimer, the yields of these two types of excimer emission are much less in this polymer LB film compared with those in a LB film of fatty acids at the same density of pyrene moieties in a layer.

In LB films of fatty acids, Yamazaki et al.[3] reported that the excitation spectrum monitored at 474 nm shifts to the red side about 2 nm, compared to that monitored at the monomer emission band. Figure 4 also shows the excitation spectra of a 20-layer LB film of P5 monitored at 375 nm. As shown in Figure 4, the excitation spectra show the same peak position as the UV absorption spectra. The excitation spectra are not much different for each polymer having different pyrene contents, and there is no spectral shift even if the spectra are monitored at 420, 470, or 375 nm. Further analysis of the excimer formation process was carried out by the time-resolved spectroscopy. Figure 5 shows the spectra of a 20-layer film of P5. Each spectrum is normalized to the maximum intensity. In the region 0–1 ns, the monomer emission was observed at 375 nm as its peak and the excimer emission was very weak. The fraction of the excimer gradually increased with time. This shows that the excimer is formed by the energy transfer from the monomer state to excimer-forming sites.

For a fatty acid LB film, the following facts have been elucidated in time-resolved fluorescence spectroscopy.[3] (a) In the short time region earlier than 2 ns, the abnormal dimer emission band appears at 4 nm to the red side, compared with the monomer band. (b) The rise of excimer emission at 470 nm is observed with the disappearance of this dimer band. The time-resolved spectra in an early time range are also shown in the right side of Figure 5. In our polymer LB films, there was no spectral shift either

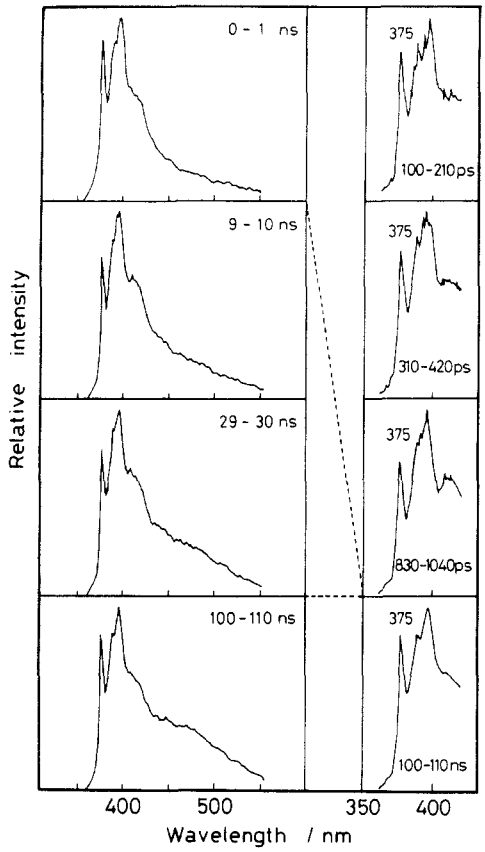

Figure 5. Time-resolved fluorescence spectra of a 20-layer LB film of P5. The excitation wavelength is 315 nm. Time zero corresponds to the time when the excitation laser pulse shows the maximum intensity.

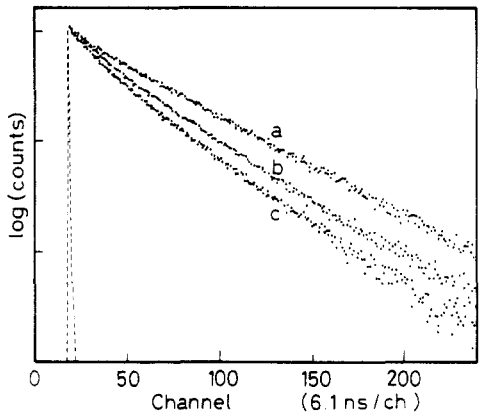

Figure 6. Fluorescence decay of the monomer emission of pyrene chromophore in 6-layer polymer LB films: (a) P1, (b) P4, and (c) P5.

in the short time region before 1 ns or in the long time region after 100 ns. Consequently, the dimer band was observed neither in the excitation spectra nor in the time-resolved fluorescence spectra, and this shows that there is no interaction between the ground states of pyrene moieties in polymer LB films.

Evaluation of Plane Density of Excimer-Forming Sites. Decay curve analysis gives further information on the energy-transfer processes from the excited monomer state to the excimer-forming sites. Figure 6 shows the monomer fluorescence decay curve of 6-layer films. Below a few percentage of pyrene moiety, the decay curves are the same as that of P2 and show single-exponential behavior, but with the increase of pyrene concentration, the fluorescence decay becomes fast and nonexponential as the result of quenching by excimer-forming sites. These

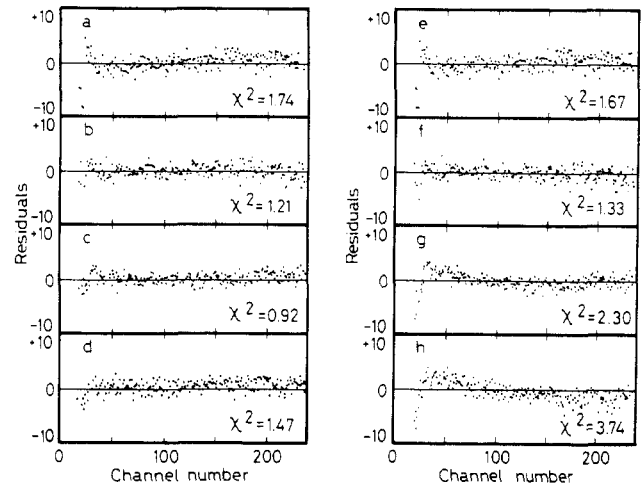

Figure 7. Plot of residuals of decay curve fitting by the Förster energy-transfer model. Residuals for 6-layer films of (a) P2, (b) P3, (c) P4, and (d) P5 analyzed by a 3-dimensional energy-transfer model and residuals of (e) P2, (f) P3, (g) P4, and (h) P5 analyzed by a 2-dimensional energy-transfer model. The number of counts in the peak channel is 10 000, and the numerals in the right side of each figure are the mean square of residuals.

decay curves are analyzed by the Förster type transfer model, which is shown by eq 1[35-37] where T_D is the lifetime

$$I(t) = I_1 \exp[-t/T_D - 2g(t/T_D)^{d/6}] + I_2 \exp(-t/T_D) \quad (1)$$

$$g = (2/3)n_A(\pi^{1/2}R_{DA})^d$$

of the donor fluorescence without any quenching processes, R_{DA} (cm) is the Förster radius between donor and acceptor chromophores, n_A is the number of acceptors (cm^{-d}) in unit area, and d is the dimension of the model; d = 2 or 3 in this study. The lifetime of P2, which has no excimer-forming site, was substituted for T_D (T_D = 280 ns). For R_{DA}, the Förster radius between pyrene moieties was used (R_{DA} = 1.1 nm).[38] The second term shows the contribution of isolated monomer decay: the monomer emission was reported to be observed in LB films of fatty acids as the component of the lifetime T_D since the pyrene moieties are in a fractal-like distribution.[3] In the system of polymer LB films, I_2 should be set to zero in order to obtain a good fit with the observed decay curves. Namely, pyrene moieties distribute so uniformly that there is no isolated monomer state in this system.

Parts a–d and e–h of Figure 7 show the plots of the residuals of decay curve fitting by the 3-dimensional model and the 2-dimensional model, respectively. The plots are for 6-layer films of P2–P5 from the top to the bottom, respectively. In the 2-dimensional analysis the mean square of the residuals[39] becomes large with an increase of pyrene concentrations; especially large deviations are observed in the short time region. On the contrary, 3-dimensional analysis can be used to stimulate the data for all the samples. This shows that the energy transfer occurs 3-dimensionally even in 6-layer films.

Next, the trap densities in a plane for 2-layer films of each sample were evaluated by 2-dimensional analysis. The results are shown in Table II. The fluorescence for P2 and P3 was not quenched enough to obtain an accurate value. The obtained values for P4 and P5 are of the order of 10^{12} cm^{-2}. An excimer site consists of two pyrene moieties. Compared with the chromophore density of pyrene moieties, excimer-forming sites are formed by one-third of the pyrene moieties for P4 and by half of the pyrene

Table II
Plane Densities of a Pyrene Chromophore and of an Excimer-Forming Site

sample	pyrene chromophore, 10^{12} cm^{-2}	excimer-forming site, 10^{12} cm^{-2}
P2	5.8	
P3	12.7	
P4	24.3	3.5
P5	34.7	6.8

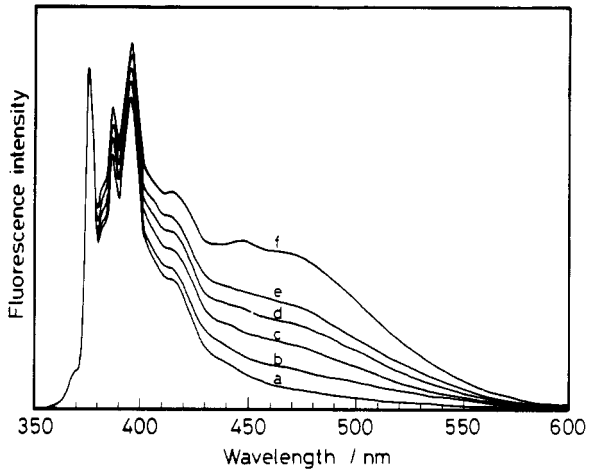

Figure 8. Fluorescence spectra of spin-coated film and polymer LB films of P5 at various numbers of transferred layers. Samples of (a) 2-, (b) 4-, (c) 6-, (d) 12-, and (e) 20-layer films and (f) a spin-coated film.

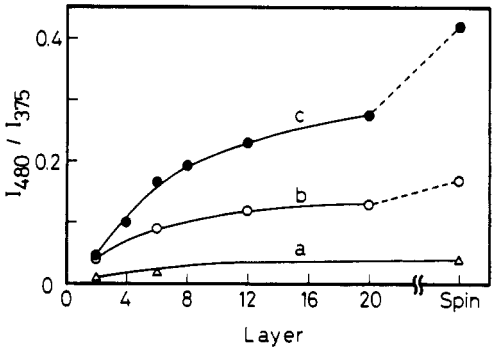

Figure 9. Ratio of excimer emission at 480 nm to the monomer emission at 375 nm as a function of the number of layers: (a) P3, (b) P4, and (c) P5.

moieties for P5. These values are one-fifth of the excimer density in the fatty acid LB films and are close to the numbers expected for a random distribution of the chromophore.[3] This shows that the chromophore distribution in polymer LB films is very uniform. Because pyrene moieties are linked to the polymer chain with covalent bonds, the statistically random distribution is attained in the polymer LB films.

Effect of Layer Number on Energy-Transfer Behavior. Figure 8 shows the fluorescence spectra of LB films of P5 for various numbers of transferred layers. The relative intensity of excimer fluorescence against the monomer emission increases with the increase of number of layers and the ratio approaches that of the spin-coated film. For comparison of the excimer formation efficiency in various pyrene concentrations, the ratio of fluorescence intensity at 480 nm (excimer emission) to that at 375 nm (monomer emission) was plotted against the number of layers in Figure 9.

The ratio for P3 is initially small, and there is no marked change with the increase of number of layers. On the contrary, the ratio for P5 increases with an increase of the

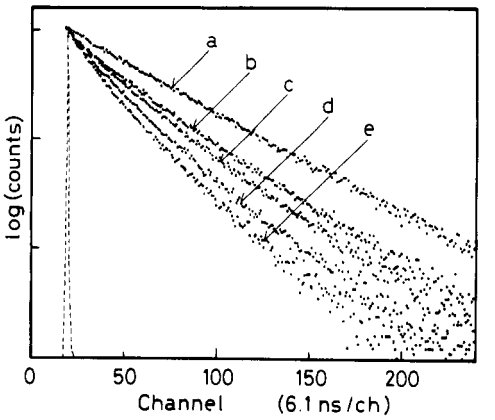

Figure 10. Fluorescence decay of the monomer emission in polymer LB films of P5 at various transferred layers: (b) 2-, (c) 6-, (d) 12-, and (e) 20-layer films. The decay a shows the fluorescence decay of a 6-layer film of P2 as the intrinsic monomer decay of pyrene without a quenching site.

Table III
Residuals of Fluorescence Decay Analysis for P5 by the Förster Energy-Transfer Model

no. of layers	χ^2 2-dimensional	χ^2 3-dimensional
2	1.13	1.01
4	1.97	1.12
6	3.74	1.47
8	6.87	2.12
12	10.7	3.48
20	14.4	4.51

number of layers and there is still a difference between the 12-layer film and the 20-layer film. The LB films of P4 show the same tendency, though the change is somehow slower than that of P5. This shows that the interlayer interaction of the excited state exists beyond several layers. The thickness of the monolayer is reported to be 1.05 nm by Ogata for poly(vinyl octal).[25] The phenomenon that the excimer formation efficiency increases with the increase of number of layers even over 12 layers cannot be explained by the model of one-step energy transfer, because the Förster radius between pyrene moieties is only 1.1 nm. There are probably a few steps of energy migration between pyrene moieties before energy transfer to the excimer-forming sites: efficient energy transfer to excimer-forming sites becomes feasible by the assistance of the energy migration from the neighboring layers.

The fluorescence decay curves for P4 and P5 at the monomer band depend on the number of layers too. Figure 10 shows the decay curves for P5. Curve a shows the fluorescence decay for a 6-layer film of P2, which gives the intrinsic lifetime of pyrene without a quenching site. The 2-layer film of P5 is clearly quenched by excimer-forming sites. The lifetime decreases with an increase of the number of layers and there is still a difference between 12-layer and 20-layer films.

Table III shows the mean square of the residuals in the analysis of the monomer fluorescence by the Förster model. Since the 2-layer film is not quenched sufficiently, the decay curve can be fitted with either a 2-dimensional or 3-dimensional model and these are not so different in the mean square of the residuals. For the 4-layer and 6-layer films, the decay curves can be reproduced only by a 3-dimensional model, because the excited states are quenched by excimer-forming sites located in the adjacent layers. Although the further layered systems are regarded as a 3-dimensional distribution of the chromophore, the fluorescence decay curves of 12- and 20-layer films cannot

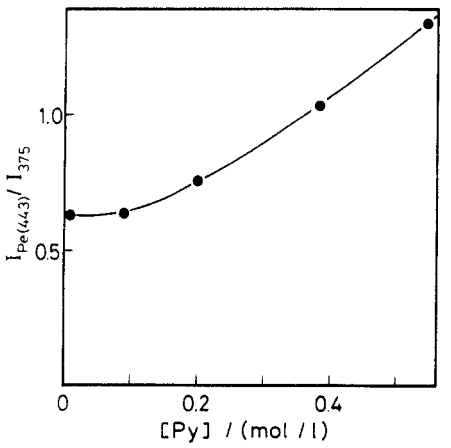

Figure 11. Ratio of perylene emission at 443 nm to pyrene monomer emission at 375 nm for the perylene-doped spin-coated film. The perylene concentration is 1.9 mmol/L for all the samples.

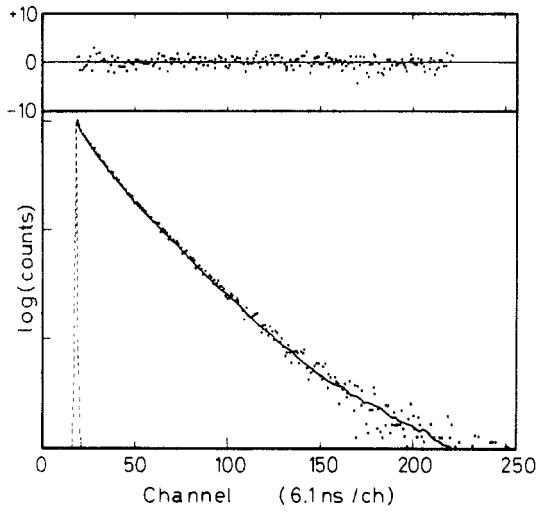

Figure 12. Fluorescence decay analysis for a 20-layer film of P5 by the Yokota–Tanimoto Padé model.

be fitted even by the 3-dimensional model: the residuals are large. The observed curves, the log (counts) vs time plots, show less downward curvature than the curves calculated by the 3-dimensional model. This behavior can be explained by the existence of energy migration between pyrene moieties. In the solid state, the relaxation process of each chromophore is different, depending on the location to the quenching site, but energy migration makes the process uniform, since spatial diffusion of excitation energy becomes possible.

Energy Migration between Pyrene Moieties. In order to confirm the existence of energy migration among pyrene moieties, perylene-doped films of each polymer were prepared by the spin-coating method. Perylene is a good acceptor for pyrene: the Förster radius from pyrene to perylene is about 3.3 nm.[38] The concentration of perylene was kept the same for all polymers. If the energy migration between pyrene moieties does not occur, the transfer efficiency from pyrene to perylene should be independent of the pyrene concentrations and be constant. Figure 11 shows the ratio of fluorescence intensity of perylene emission to that of pyrene emission against pyrene concentrations. For P1 and P2 the ratios are almost the same. Then this means that the excitation energy does not migrate between pyrene moieties in low chromophore concentrations. However, as the pyrene concentration increases over P3, the sensitized fluorescence of perylene increases. The result shows that energy migration takes place between pyrene moieties in the concentrations higher than 0.2 mol/L, which corresponds to the concentration in P3 bulk. The spin-coated films are thick enough (ca. 300 nm) to be regarded as a limit of a multilayered LB film. Then, it is expected that, for the samples of higher pyrene concentration than P3, the energy migration also occurs in multilayered LB films. Actually, the fluorescence decay of the LB film of P5 shows the effect of the energy migration, as described above.

In order to estimate quantitatively the diffusion rate of singlet energy within the LB films, the fluorescence decay curve was analyzed by the Yokota–Tanimoto Padé model in which the energy diffusion process besides the Förster type transfer is taken into account. The function derived by them is[40,41]

$$I = I_0 \exp(-t/T_D) \exp(-K[A]) \quad (2)$$

$$K = (4/3)\pi^{3/2}N'(at)^{1/2}B$$

$$B = [(1 + 10.87x + 15.50x^2)/(1 + 8.743x)]^{3/4}$$

$$a = R_{DA}{}^6/T_D$$

$$x = Da^{-1/3}t^{2/3}$$

where [A] is the molar acceptor concentration, N' is Avogadro's number per millimole, and D is the diffusion coefficient of excitation energy. For the decay curves of 20-layer films of P2 and P3, the model of the Förster type transfer (eq 1 or $D = 0$ in eq 2) fits well, and then the migration does not occur in these pyrene concentrations. The decay curves of 20-layer films of P4 and P5, which were impossible to be fit by the Förster model, were successfully fitted by this model. But, the result of P4 is inaccurate because the curve fitting was possible with various pairs of D and trap concentration. Figure 12 shows the curve fitting for the 20-layer film of P5 with the Yokota–Tanimoto Padé model. The mean square of residuals is 1.39; i.e., the decay curve could be reproduced satisfactorily. The obtained diffusion coefficient is 1×10^{-8} cm^2 s^{-1}, and the trap density is 180 mmol L^{-1}. This shows that the energy migration between pyrene moieties takes an important role in the energy-trapping process, although the migration rate is rather small.

Conclusion

Mono- and multilayered polymer films containing pyrene chromophore have been prepared by the LB method. The use of copolymers gives another structural variation for LB films. Besides interlayer arrangement, the lateral organization becomes adjustable with the design of polymer composition. In the present study, the built-up layered systems (2-dimensional or quasi 3-dimensional systems) have been investigated from a photophysical standpoint. Some unique characteristics have been demonstrated by fluorescence spectroscopy, especially by the time-resolved measurements. The results are summarized as follows.

(1) Poly(vinyl octal) is a useful base polymer to make the LB films containing various photofunctional chromophores. The monolayer on the water surface is easily built up on substrates, even if a considerable fraction of octyl units is replaced by pyrene units.

(2) A uniform chromophore distribution can be realized by the copolymer. Excimer formation and aggregation of pyrene moieties in the ground state are considerably suppressed, compared with the LB films of fatty acids.

(3) Plane densities of excimer-forming sites were evaluated by the decay curve analysis. The result shows that pyrene moieties are in a statistically random distribution in a 2-dimensional film.

(4) Although the Förster radius of pyrene chromophore is very small, interlayer energy migration is observed at high pyrene concentrations. The thickness of each layer is only 1 nm, which is comparable to the Förster radius. This results in an efficient energy flow through adjacent layers.

Acknowledgment. We express our thanks to Prof. Hiroshi Hada and Yoshiro Yonezawa of Kyoto University for their kind guidance on the Langmuir–Blodgett technique. This work was partially supported by a Grant-in-Aid for Scientific Research (No. 01550692) and a Grant-in-Aid for Scientific Research on Priority Areas, New Functionality Materials-Design, Preparation and Control (No. 01604567), from the Ministry of Education, Science and Culture of Japan.

References and Notes

(1) (a) Kuhn, H.; Möbius, D.; Bücher, H. In *Physical Methods of Chemistry*; Weissberger, A., Rossiter, B. W., Ed.; Wiley: New York, 1972; Vol. 1, Part 3B, p 577. (b) Möbius, D. *Ber. Bunsen-Ges. Phys. Chem.* **1978**, *82*, 848. (c) Kuhn, H. *J. Photochem.* **1979**, *10*, 111. (d) Kuhn, H. *Pure Appl. Chem.* **1981**, *53*, 2105.
(2) (a) Tamai, N.; Yamazaki, T.; Yamazaki, I. *J. Phys. Chem.* **1987**, *91*, 841. (b) Tamai, N.; Yamazaki, T.; Yamazaki, I. *Chem. Phys. Lett.* **1988**, *147*, 25. (c) Yamazaki, I.; Tamai, N.; Yamazaki, T.; Murakami, A.; Mimuro, M.; Fujita, Y. *J. Phys. Chem.* **1988**, *92*, 5035.
(3) (a) Yamazaki, T.; Tamai, N.; Yamazaki, I. *Chem. Phys. Lett.* **1986**, *124*, 326. (b) Yamazaki, I.; Tamai, N.; Yamazaki, T. *J. Phys. Chem.* **1987**, *91*, 3572.
(4) Cemel, A.; Fort, T., Jr.; Lando, J. B. *J. Polym. Sci., Polym. Chem. Ed.* **1972**, *10*, 2061.
(5) (a) Fukuda, K.; Shiozawa, T. *Thin Solid Films* **1980**, *68*, 55. (b) Fukuda, K.; Shibasaki, Y.; Nakahara, H. *Thin Solid Films* **1983**, *99*, 87.
(6) (a) Barraud, A.; Rosilio, C.; Ruaudel-Teixier, A. *Thin Solid Films* **1980**, *68*, 91. (b) Barraud, A. *Thin Solid Films* **1983**, *99*, 317.
(7) Sarkar, M.; Lando, J. B. *Thin Solid Films* **1983**, *99*, 119.
(8) Miyashita, T.; Yoshida, H.; Murakata, T.; Matsuda, M. *Polymer* **1987**, *28*, 311.
(9) (a) Tieke, B.; Graf, H.-J.; Wegner, G.; Naegele, B.; Ringsdorf, H.; Banerjie, A.; Day, D.; Lando, J. B. *Colloid Polym. Sci.* **1977**, *255*, 521. (b) Lieser, G.; Tieke, B.; Wegner, G. *Thin Solid Films* **1980**, *68*, 77.
(10) Laschewsky, A.; Ringsdorf, H.; Schmidt, G. *Polymer* **1988**, *29*, 448.
(11) Uchida, M.; Tanizaki, T.; Kunitake, T.; Kajiyama, T. *Macromolecules* **1989**, *22*, 2381.
(12) Halperin, K.; Peng, J. B.; Sailor, M.; Gadwood, R.; Ketterson, J. B.; Dutta, P. *J. Polym. Sci., Part B: Polym. Phys.* **1989**, 27, 1289.
(13) Breton, M. *J. Macromol. Sci., Rev. Macromol. Chem.* **1981**, *C21* (1), 61.
(14) (a) Takenaka, T.; Harada, K.; Matsumoto, M. *J. Colloid Interface Sci.* **1980**, *73*, 569. (b) Takeda, F.; Matsumoto, M.; Takenaka, T.; Fujiyoshi, Y. *J. Colloid Interface Sci.* **1981**, *84*, 220.
(15) (a) Tredgold, R. H.; Winter, C. S. *J. Phys. D: Appl. Phys.* **1982**, *15*, L55. (b) Tredgold, R. H.; Winter, C. S. *Thin Solid Films* **1983**, *99*, 81. (c) Vickers, A. J.; Tredgold, R. H.; Hodge, P.; Khoshdel, E.; Girling, I. *Thin Solid Films* **1985**, *134*, 43. (d) Winter, C. S.; Tredgold, R. H.; Vickers, A. J.; Khoshdel, E.; Hodge, P. *Thin Solid Films* **1985**, *134*, 49. (e) Tredgold, R. H. *Thin Solid Films* **1987**, *152*, 223.
(16) Naito, K. *J. Colloid Interface Sci.* **1989**, *131*, 218.
(17) (a) Kakimoto, M.; Suzuki, M.; Konishi, T.; Imai, Y.; Iwamoto, M.; Hino, T. *Chem. Lett.* **1986**, 823. (b) Nishikata, Y.; Kakimoto, M.; Imai, Y. *J. Chem. Soc., Chem. Commun.* **1988**, 1040.
(18) (a) Kawaguchi, T.; Nakahara, H. *J. Colloid Interface Sci.* **1985**, *104*, 290. (b) Kawaguchi, T.; Nakahara, H.; Fukuda, K. *Thin Solid Films* **1985**, 133, 29.
(19) (a) Matsumoto, M.; Itoh, T.; Miyamoto, T. In *Cellulose and Its Utilization*; Inagaki, H., Phillips, G. O., Ed.; Elsevier: New York, in press. (b) Itoh, T.; Suzuki, H.; Matsumoto, M.; Miyamoto, T. In *New Functionalization of Cellulosics*; Phillips, G. O., Williams, P. A., Ed.; Ellis Horwood: Chichester, U.K., in press.
(20) Mumby, S. J.; Swalen, J. D.; Rabolt, J. F. *Macromolecules* **1986**, *19*, 1054.
(21) (a) Laschewsky, A.; Ringsdolf, H.; Schmidt, G.; Schneider, J. *J. Am. Chem. Soc.* **1987**, *109*, 788. (b) Ringsdolf, H.; Schmidt, G.; Schneider, J. *Thin Solid Films* **1987**, *152*, 207. (c) Schneider, J.; Ringsdolf, H.; Rabolt, J. F. *Macromolecules* **1989**, *22*, 205. (d) Schneider, J.; Erdelen, C.; Ringsdolf, H.; Rabolt, J. F. *Macromolecules* **1989**, *22*, 3475.
(22) Carpenter, M. M.; Prasad, P. N.; Griffin, A. C. *Thin Solid Films* **1988**, *161*, 315.
(23) (a) Murakata, T.; Miyashita, T.; Matsuda, M. *Macromolecules* **1988**, *21*, 2730. (b) Murakata, T.; Miyashita, T.; Matsuda, M. *Macromolecules* **1989**, *22*, 2706.
(24) (a) Seki, T.; Ichimura, K. *Polym. Commun.* **1989**, *30*, 108. Seki, T.; Tamaki, T.; Suzuki, Y.; Kawanishi, Y.; Ichimura, K.; Aoki, K. *Macromolecules* **1989**, *22*, 3505.
(25) (a) Engel, A. K.; Yoden, T.; Sanui, K.; Ogata. N. *J. Am. Chem. Soc.* **1985**, *107*, 8308. (b) Oguchi, K.; Yoden, T.; Sanui, K.; Ogata, N. *Polym. J.* **1986**, *18*, 887. (c) Watanabe, M.; Kosaka, Y.; Sanui, K.; Ogata, N.; Oguchi, K.; Yoden, T. *Macromolecules* **1987**, *20*, 452. (d) Watanabe, M.; Kosaka, Y.; Oguchi, K.; Sanui, K.; Ogata, N. *Macromolecules* **1988**, *21*, 2997. (e) Oguchi, K.; Yoden, T.; Kosaka, Y.; Watanabe, M.; Sanui, K.; Ogata, N. *Thin Solid Films* **1988**, *161*, 305.
(26) (a) Ito, S.; Okubo, H.; Ohmori, S.; Yamamoto, M. *Thin Solid Films* **1989**, *179*, 445. (b) Ohmori, S.; Ito, S.; Yamamoto, M.; Yonezawa, Y.; Hada, H. *J. Chem. Soc., Chem. Commun.* **1989**, 1293.
(27) (a) Ito, S.; Yamashita, K.; Yamamoto, M.; Nishijima, Y. *Chem. Phys. Lett.* **1985**, *117*, 171. (b) Ohmori, S.; Ito, S.; Yamamoto, M. *Ber. Bunsen-Ges. Phys. Chem.* **1989**, *93*, 815.
(28) O'Connor, D. P.; Phillips, D. *Time-Correlated Single Photon Counting*; Academic: London, 1984.
(29) Yamazaki, I.; Tamai, N.; Kume, H.; Tsuchiya, H.; Oba, K. *Rev. Sci. Instrum.* **1985**, *56*, 1187.
(30) Spencer, R. D.; Weber, G. *J. Chem. Phys.* **1970**, *52*, 1654.
(31) Crisp, D. J. *J. Colloid Sci.* **1946**, *1*, 49.
(32) Johnson, G. E. *Macromolecules* **1980**, *13*, 839.
(33) (a) Fujihira, M.; Nishiyama, K.; Hamaguchi, Y. *J. Chem. Soc., Chem. Commun.* **1986**, 823. (b) Fujihira, M.; Yamada, H. *Thin Solids Films* **1988**, *160*, 125. (c) Fujihira, M.; Nishiyama, K.; Aoki, K. *Thin Solid Films* **1988**, *160*, 317.
(34) Kinnunen, P. K. J.; Tulkki, A.-P.; Lemmetyinen, H.; Paakkola, J.; Virtanen, J. A. *Chem. Phys. Lett.* **1987**, *136*, 539.
(35) Förster, Th. *Z. Naturforsch.* **1949**, *4A*, 321.
(36) Hauser, M.; Klein, U. K. A.; Gösele, U. *Z. Phys. Chem. (Munich)* **1976**, *101*, S255.
(37) Klafter, J.; Blumen, A. *J. Chem. Phys.* **1984**, *80*, 875.
(38) Berlman, I. B. *Energy Transfer Parameter of Aromatic Compounds*; Academic: New York, 1973.
(39) The mean square of residuals (χ^2) is calculated by the equation

$$\chi^2 = \sum_{i=n_1}^{n_2} [I_o(t_i) - Y(t_i)]^2 / [(n_2 - n_1 + 1 - p) I_o(t_i)]$$

where $I_o(t_i)$ is the observed decay function, $Y(t_i)$ is the calculated fitting function, and p is the number of fitting parameters.[28]
(40) Yokota, M.; Tanimoto, O. *J. Phys. Soc. Jpn.* **1967**, *22*, 779.
(41) Renschler, C. L.; Faulkner, L. R. *J. Am. Chem. Soc.* **1982**, *104*, 3315.

Registry No. Perylene, 198-55-0.